Application of pervaporation in the bio-production of glycerol carbonate

Wenqi Li[a], Ramesh Sreerangappa[b], Julien Estager[c], Jean-Christophe M. Monbaliu[d], Damien P. Debecker[b], Patricia Luis[a]*

[a] Materials & Process Engineering (iMMC-IMAP), Université catholique de Louvain, Place Sainte Barbe 2, 1348 Louvain-la-Neuve, Belgium

[b] Institute of Condensed Matter and Nanoscience (IMCN), Université catholique de Louvain, Place Louis Pasteur, 1, box L4.01.09, 1348 Louvain la-Neuve, Belgium

[c] Certech, Centre de ressources technologiques en chimie, Rue Jules Bordet, Zone Industrielle C, 7180 Seneffe, Belgium

[d] Center for Integrated Technology and Organic Synthesis, Department of Chemistry, University of Liège, B-4000 Liège (Sart Tilman), Belgium

* Tel: +32 16 322348; Fax: +32 16 322991; Email: patricia.luis@uclouvain.be

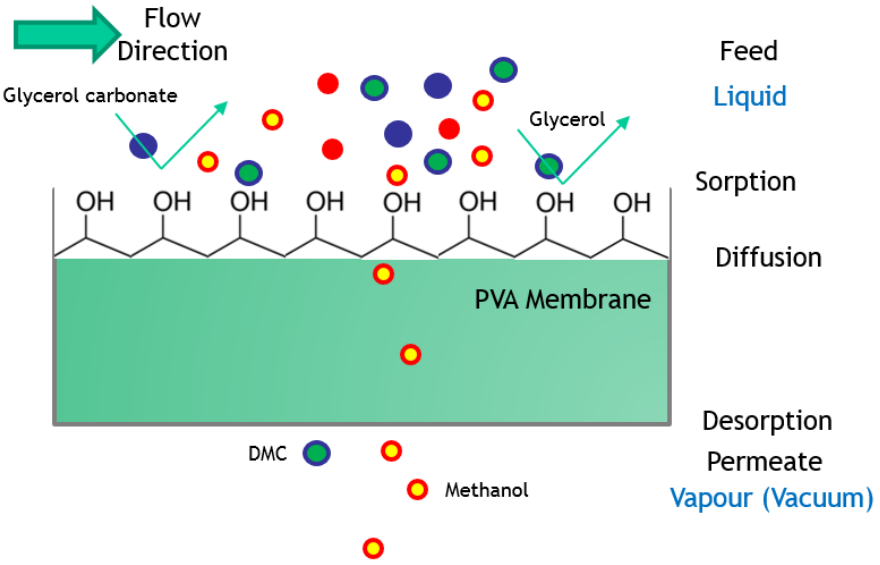

Abstract

Glycerol carbonate is a platform molecule with a large range of applications. It can be synthesized from glycerol by transesterification with dimethyl carbonate, which is considered a bio-based path of synthesis since glycerol is originated during the production of biodiesel. The purification of the reaction products is quite challenging and costly using conventional separation technology, since methanol (by-product) and dimethyl carbonate (in excess) form an azeotropic mixture. In this work, pervaporation is presented as a technological alternative to separate the multicomponent mixture composed of methanol, glycerol, dimethyl carbonate and glycerol carbonate, *i.e* reactants and products of the reaction of synthesis of glycerol carbonate. The separation performance of four commercial membranes namely PERVAP 1255-30, PERVAP 4155-40, PERVAP 1255-50, PERVAP 4155-80 from Sulzer Chemtech, Switzerland, was evaluated. The effect of temperature (30°C, 45°C, and 60°C ±2 °C) on the separation performance was also studied in terms of transmembrane flux, separation factor, permeance and selectivity. Results show that the membranes reject glycerol and glycerol carbonate completely (not detected in the permeate), and permeate methanol and dimethyl carbonate, with higher selectivity for methanol. In addition, the performance of pervaporation separation was compared with that obtained by distillation via the McCabe-Thiele diagram, showing the technical advantage of pervaporation.

Keywords: Glycerol carbonate; transesterification reaction; Pervaporation; Activation energy; Activity; Azeotrope

1. Introduction

The development of renewable energy sources is critical because of the energy crisis caused by the depletion of petroleum reserves and the environmental concerns associated with CO_2 emissions. The production of biodiesel is nowadays one of the most important sources of bioenergy, and it has been growing dramatically as a sulfur-free, non-toxic and biodegradable additive for fuels.[1] The production in 2006 reached 6.5 billion liters.[2] As a consequence, the production of biobased glycerol - a co-product of biodiesel production, representing 10 wt% of the total its production[3–5]

– has also encountered a massive increase, leading to a dramatic decrease of its value in the market from 900-950 USD/ton in 2013 to 240 USD/ton in 2014.[6] Extensive research has been performed to convert glycerol into other value-added chemicals such as 1,3-propanediol, polyglycerols, polyurethanes, lactates, acrolein or bioethanol.[7–13] Glycerol carbonate is one of these products and can be extremely valuable because of its low toxicity, good water solubility and biodegradability, and it can be also used as an intermediate for the production of other chemicals. Some of its applications include: solvent in the manufacture of cosmetics and pharmaceutics, lubricating oil, solvent in lithium ion batteries and surfactant.[14,15] Different routes can lead to the synthesis of glycerol carbonate and they have been reviewed quite recently.[14] For example, glycerol carbonate can be prepared from glycerol and phosgene using metallic catalysts, but this process is obviously difficult to implement due to toxicity issues.[16] Another route consist in a carbonation reaction between urea and glycerol under low pressure (40-50 mbar) to shift the equilibrium and generate glycerol carbonate. The separation of the by-product ammonia is then necessary.[17] Glycerol can also react with CO_2 using zeolite/Sn catalysts to obtain glycerol carbonate, but the conversion is quite low (max. 32% with catalyst Purosiv).[18] Finally, one direct way to produce glycerol carbonate is *via* a transesterification reaction of glycerol generally using either ethylene carbonate or dimethyl carbonate as reactants. When the former compound is used[19,20], the separation can be difficult because the by-product (ethylene glycol) has high boiling point (197.3 °C).[21] On the other hand, the use of dimethyl carbonate (DMC) lead to methanol as a by-product, as indicated in the schema 1.[21–29] This transesterification reaction is of interest because it is a simple route to produce glycerol carbonate, and dimethyl carbonate is a renewable green chemical with environmentally sustainable applications.[30–32]

Schema 1. Transesterification reaction of glycerol and dimethyl carbonate to produce glycerol carbonate. Methanol is considered byproduct in this reaction.

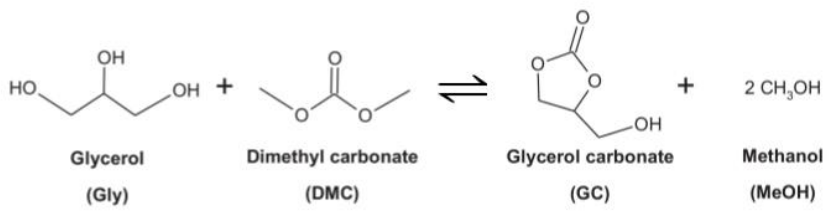

Since it is a transesterification reaction, the production yield is enhanced by using an excess of

dimethyl carbonate. The boiling point of dimethyl carbonate and methanol are 90.3 °C and 64.7 °C respectively. Thus, the use of distillation as a separation method seems to be more appealing here than for the glycerol carbonate synthesis involving ethylene carbonate (b.p. 243°C under atmospheric pressure) and ethylene glycol (197.3°C). In this case, however, the major challenge is the formation of an azeotropic mixture at a composition ratio of 30/70 (wt%/wt%) in DMC/methanol, making distillation energetically (and economically) very unfavorable.

Pervaporation is a promising membrane-based technology for the separation of liquid mixtures in which vacuum is applied in the permeate side to enhance the differences in partial pressure between the feed and permeate sides. If compared to distillation or evaporation, pervaporation is a low energy consumption process.[33,34] Several studies confirm the energetic advantage of using pervaporation instead of distillation or as hybrid process.[35] If compared to solvent extraction (yet another low energy consumption process), it does not involve the use of an often toxic and flammable and usually expensive solvent. This technology has been applied to different areas, such as organic-organic separations[36], waste water treatment[37], esterification reactions[38,39] or alcohol dehydration[40]. Noteworthy, pervaporation can improve the reaction yield *via* the selective removal of one of the product in the reaction mixture, leading to a shift of the equilibrium according to the Le Chatelier-Braum principle. This technology has been proposed in many studies as an alternative technology to separate azeotrope mixtures because the separation is not based on the thermodynamic equilibrium but only depends on the interaction of a membrane and the permeants. The membrane acts as a barrier to provide selectivity for the compounds and determine which compounds can diffuse through it according to their affinity with the membrane. The driving force is the gradient of chemical potential on both sides of the membrane. Hence, the sorption and diffusion of components within the membrane determines the permeate composition.[41]

In this work, pervaporation is proposed as the technology to separate the transesterification mixture involved in the production of glycerol carbonate from glycerol and DMC. The performance of four commercial membranes is evaluated from the results of transmembrane flux, separation factor, permeance, selectivity, and a comparison with distillation via the McCabe-Thiele diagram.

2. Experimental section

2.1 Chemicals

Glycerol (bidistilled, VWR PROLABO Chemicals, France, purity ≥ 99.5%) and dimethyl carbonate (ThermoFisher (Kandel) GmbH, Germany, purity ≥ 99%) are used as reagents of the transesterification reaction (schema 1) in order to produce the quaternary mixture that will be introduced in the pervaporation unit as feed solution. Sodium aluminate $NaAlO_2$ (Carlo Erba, Italy, purity ≥98) is used as catalyst for that transesterification reaction.[22]

2.2 Membranes

The commercial membranes Pervap 1255-30, 4155-40, 1255-50 and 4155-80 manufactured by Sulzer Chemtech GmbH (Switzerland) were studied. According to the information obtained from the supplier, they are composite membranes containing three layers. The top layer is active layer of the membranes containing polyvinyl alcohol (PVA) with a thickness of 0.5-5 µm. In the middle, a thickness of 70-100 µm porous support layer is made of polyacrylonitrile. Finally, at the bottom of the membrane, a thickness of 100-150 µm mechanical support layer composes of polyphenylene sulfide polymer. According to the supplier, the PVA content in the different types of membranes studied is different. In comparison, the 4155-80 membrane contains more PVA than the other ones, followed by 1255-50, 4155-40 and 1255-30. The membranes were immersed in the feed solution for 24 hours before running the pervaporation experiment.

In order to foresee the membrane affinity with the components in the feed solution, a preliminary study of Hansen solubility parameters was performed (see Appendix A4). As result, it was observed that methanol could have high permeation in the PVA membrane. Thus, coupling effects may occur due to the sorption of components in the PVA membrane.

2.3 Transesterification of glycerol with DMC

The feed solution for pervaporation separation corresponds to the mixture of the transesterification reaction between glycerol and dimethyl carbonate. The initial mixture before the reaction starts is biphasic (mixture of glycerol and DMC). The molar fraction of the initial mixture is 1:2 in glycerol/DMC; an excess of dimethyl carbonate is used to enhance the kinetics of

the reaction and to force the equilibrium towards the formation of glycerol carbonate. Noteworthy, glycerol is a relatively viscous liquid, and using more dimethyl carbonate can improve the mixing between reagents and the catalyst. Glycerol (678.75 g), DMC (1386.74 g) and $NaAlO_2$ (18.83 g) were mixed in a 2500 mL round bottom flask glass reactor equipped with a magnetic stirrer and heated in an oil batch. The reaction was run for 30 min at 90 °C. After reaction, the mixture was filtered in order to remove the fine powder catalysts. The final concentration of filtered mixture is determined by gas chromatography (see section 2.4). After filtration, the mixture consists in a monophasic system with molar ratio of 0.075/0.291/0.193/0.44 in glycerol/DMC/glycerol carbonate/methanol. This mixture is the feed solution for the pervaporation experiments.

2.4 Gas chromatography analysis

The reaction products before and after pervaporation were analyzed by gas chromatography (GC-456 SCION BRUKER) equipped with a flame ionization detector, split/splitless injection unit and a capillary column (DB-WAX, 30 m, 0.25 mm, 0.25 m). Helium was used as the carrier gas. The injection was performed in split mode with a split ratio of 100:1. Initially, the oven temperature was set at 80°C and it was increased at the rate of 15°C /min until it reached 240°C. Then, it was maintained at this temperature for 15 min. The FID and injection temperatures were fixed at 270°C and 300°C, respectively.

2.5 Pervaporation experiments

A laboratory pervaporation equipment (unit 3'' round cell, Sulzer Chemtech GmbH, Switzerland) was used to perform the pervaporation experiments. The experimental setup is shown in Figure 1.

When the experiment started, the set-up was stabilized for two hours before the samples of permeate were collected. The feed solution (*i.e.,* mixture obtained as indicated in section 2.3) was stored in a stainless steel tank (max. 1.5 Liter). The feed solution was transported and recirculated by using a centrifugal pump with a peripheral impeller (Speck Pimpen Systemtechnik GmbH, Germany) and the flow rate was between 70-80 L/h. With this high flow rate, the estimated Reynolds number reaches a value of 12550-14334 in the membrane cell. Therefore, a turbulent flow is achieved minimizing any effect caused by concentration polarization.

The experimental temperature, which was measured in the membrane cell, was kept at 30, 45 or 60 °C (+/- 2 °C). In order to maintain desired temperatures, a heating circulator produced by Julabo model ME, Germany was used. At the permeate side of the membrane cell, a vacuum pump maintained the desired vacuum pressure (8-12 mbar). A flat sheet membrane was placed in the membrane cell; the active area of the installed membrane was 38.48 cm^2 with diameter 7.0 cm. The membrane was soaked in the feed 24 hour before the experiments started. The sample of permeate was weighed every 60 minutes. The concentrations were analyzed for the solutions sampled every 60 minutes by means of gas chromatography, as indicated in section 2.4.

The weight of permeate was measured by a balance with high precision 10^{-4} g (Mettler-Toledo, AE200, Belgium). The flux J (kg/m^2·h) was calculated as follows:

$$J = \frac{w}{\Delta t \times A} \quad (1)$$

where A is the membrane area (m^2), Δt is the period of collecting time (h) and w is the weight of permeate (kg). Since the concentration in the feed and permeate were measured by gas chromatography, therefore, the partial flux (J_i: kg/m^2·h) can be calculated:

$$J_i = J \times y_i \quad (2)$$

in this equation y_j is molar fraction of component i in the permeate.

The permeance ($\frac{P_i}{l}$: GPU) of component i is the partial flux of component i divided by its driving force[42]:

$$\frac{P_i}{l} = \frac{J_i}{(x_i \times \gamma_i \times P_i^0 - y_i \times P_p)} \quad (3)$$

The vapor pressures P_i^0 (atm) are calculated by Aspen Plus.[43] The activity coefficients at different temperatures were calculated by the UNIFAC method; the group and group parameters required by UNIFAC for the studied components in this work can be found in the literature.[44,45] The vacuum pressure P_p (atm) was measured during the experiment. From equation 3, it can be seen that the influence of driving force is therefore eliminated.

The separation factor (β) is calculated by equation 4. It is the ratio between the molar concentration of each component (i, j) in the permeate (y_i, y_j) and feed (x_i, x_j) solutions.

$$\beta_{i/j} = \frac{y_i/y_j}{x_i/x_j} \quad (4)$$

The selectivity (α) of the membrane is calculate as the ratio of permeances or permeabilities:

$$\alpha_{i/j} = \frac{P_i/l}{P_j/l} = \frac{P_i}{P_j} \quad (5)$$

184 If selectivity is larger than 1, this means that the membrane is more favorable to permeate the
185 component *i* than the component *j*.

186 The temperature effect on the transmembrane flux can be investigated by an Arrhenius-type
187 equation:

$$J = J_0 \exp\left(-\frac{E_P}{RT}\right) \quad (6)$$

188 which can be also written as

$$\ln J_P = -\frac{E_P}{RT} + \ln J_0 \quad (7)$$

189 where E_P is the permeation activation energy (J/mol) and J is the permeation flux (kg/m^2·h), J_0 is
190 the pre-exponential factor, R is the gas constant (8.314 J/mol·K) and T is temperature (K). E_P
191 and J_0 can be calculated graphically through the fitting $\ln J_P$ vs. 1/T.

192 The permeant transport rate depends on sorption and diffusion through the membrane, therefore,
193 the permeability is expressed by the product of the diffusion coefficient D_i and the sorption
194 coefficient S_i of a component *i* in the membrane [46]:

$$P_i = D_i \times S_i \quad (8)$$

195 An Arrhenius-type equation was considered as both D_i and S_i are temperature dependent. They
196 can be determined by the following equations[47]:

$$S_i = S_{i,0} \exp\left(\frac{-\Delta H_{i,S}}{RT}\right) \quad (9)$$

$$D_i = D_{i,0} exp\left(\frac{-E_{i,D}}{RT}\right) \quad (10)$$

197 where $S_{i,0}$ and $D_{i,0}$ are the temperature-dependent constants. $\Delta H_{i,S}$ is the heat of solution and
198 $E_{i,D}$ is the activation energy for diffusion. Therefore, P_i can be written as follows:

$$P_i = D_{i,0} S_{i,0} exp\left(-\frac{\Delta H_{i,S} + E_{i,D}}{RT}\right) \quad (11)$$

199 The activation energy of permeation is expressed by the following equation[47]:

$$E_{i,P} = E_{i,D} + \Delta H_{i,S} \quad (12)$$

200 The activation energy of permeation was estimated by an Arrhenius-type equation:

$$\frac{P_i}{l} = \frac{P_{i,\infty}}{l} \times exp\left(-\frac{1000 \times E_{i,P}}{RT}\right) \quad (13)$$

201 where P_i/l is the permeance of component *i*, and $P_{i,\infty}/l$ is the pre-exponential factor. The

temperature effect on permeance can be thus interpreted in terms of energy of activation. From the equations above, it can be observed that an increase of temperature would improve diffusion and, as consequence, the activation energy of diffusion $E_{i,D}$ is usually positive.

3. Results and discussion

3.1 Pervaporation performance

The total transmembrane flux is shown in Figure 2 as a function of the temperature for the studied membranes. The partial flux of each component is shown in Figure 3. The overall transmembrane flux follows the trend: 1255-30>4155-40>155-50>4155-80 for all tested temperature. This could be an indication that the high degree of PVA polymer chain crossing-linking, such as in 4155-80, leads to a decrease of the transmembrane flux. Hence, the degree of cross-linking is a more important factor than the temperature effect regarding to the molecule motion within the polymer. In addition, the effect of the thickness will also have an impact on the permeation performance. The thickness of the studied membranes is different, having the membrane 1255-30 the thinnest layer and the membrane 4155-80 the thickest one. This is in agreement with the obtained results since a thicker layer would normally produce more resistance to mass transfer.

Regarding the partial flux of each component, all the membranes rejected glycerol and glycerol carbonate completely, meaning that only methanol and dimethyl carbonate can diffuse through them. In general, the partial flux of methanol is higher than that of dimethyl carbonate for all membranes. This phenomenon can be interpreted by studying the driving force. In equation 4, the term representing the driving force is $(x_i \times \gamma_i \times P_i^0 - y_i \times P_p)$. In the pervaporation process, the vacuum pressure is about 12-15 mbar, and, therefore, the term $y_i P_p$ can be neglected. The vapor pressure P_i^0 plays an important role on the driving force as well as the activity coefficient γ_i. With an increase in temperature, the vapor pressure of methanol and dimethyl carbonate increased dramatically (Table A1 in Appendix). As a result, it can be concluded that a high transmembrane flux was obtained due to a larger driving force, which is caused by a higher vapor pressure. The calculated driving force of different membranes with different experimental temperatures is given

in table A3 in the Appendix.

In addition, glycerol and glycerol carbonate were totally rejected by the membrane due to their extremely low vapor pressure (glycerol at 60 °C: $7.96X10^{-6}$ atm and glycerol carbonate at 60 °C $3.85X10^{-6}$ atm). The activity coefficient of each compound is between 1.853 and 1.091 at 60 °C (see Table A2 in Appendix); compared to the large variation of vapor pressure of each component at different temperatures, the impact of the variation of activity coefficients can be considered as very small. Therefore, the vapor pressure plays an important role on the permeation behavior.

Furthermore, the flux is clearly temperature dependent, increasing when the temperature increases except for the 4155-80 membrane. An increase of temperature may promote the thermal motion of permeant molecules, consequently, improving the diffusion. In addition, the increase of temperature leads to an increase of the motions of polymer chains and expansion of the free volume.[48] Therefore, the permeant molecules can diffuse through the cross-linked membrane easier. The temperature effect on the transmembrane flux was investigated by equation (7) and (8), which is presented in Figure 4. In Figure 4, it can be seen that the experimental data shows good linear relationship between $\ln J_P$ and 1/T. It is clearly shown that the flux of 1255-30, 4155-40 and 1255-50 membranes is temperature dependent, and they have a negative permeation activation energy E_P, which indicates that the flux increases with increasing the temperature. However, for the 4155-80 membrane, the flux is independent of temperature. This phenomenon may be explained by the highly cross-linking degree of this type of PVA membrane matrix, which leads to a limitation in the thermal motion of the polymer chains caused by the temperature change.[49]

The separation factor methanol/dimethyl carbonate is shown in Figure 5. The results show a high separation factor in all membranes, indicating a permeate rich in methanol. The lowest separation factor is higher than 4 (1255-30 membrane at 30 °C) while the highest one is around 14 (1255-50 membrane at 45 °C).

3.2 Membrane performance

The membrane performance was evaluated in terms of permeance and selectivity in order to remove the effect of the driving force of each component.[50] The results of permeance are shown

in Figure 6. At the same temperature, the permeance of membranes follows 1255-30>4155-40>1255-50>4155-80. According to the information obtained from the supplier, this could result from the different free volume of different types of polymeric membranes. The membrane 1255-30 membrane has more free volume than the membrane 4155-80, therefore, the molecules can diffuse through the membrane 1255-30 easier than the membrane 4155-80. Unfortunately, the supplier did not provide precise values concerning the free volume of the different membrane subsequently leading only to comparative conclusions.

It is observed that the permeance of methanol in each membrane is always higher than the one of dimethyl carbonate, showing that the membrane has more affinity with methanol. The functional layer of the membranes is made of polyvinyl alcohol, which contains hydroxyl function group. Methanol has a better affinity to PVA polymer due to its higher polarity than that of dimethyl carbonate. Hence, a high hydrogen bonding interaction with hydroxyl group can enhance the methanol permeation. On the other hand, the smaller molecular size of methanol can lead to a high permeation.[51] As a result, the permeation of methanol is higher than the one of dimethyl carbonate. Additionally, the study of Hansen' solubility parameter shows that methanol molecules can be sorbed by the PVA separation layer easier than dimethyl carbonate. As a consequence, more methanol molecules can diffuse through the membrane. The experimental results are in agreement with the preliminary study of Hansen' solubility parameters indicated in section Appendix A4.

Regarding to the selectivity (DMC/Methanol), results are shown in Figure 7. The lowest selectivity is around 2 (1255-30 membrane at 30 °C); a value of selectivity higher than 1 indicates that the membrane is selective towards methanol. It can be then concluded that the 1255-50 membrane operated at 45 °C is the optimal choice for the separation, both in terms of the separation factor and selectivity.

Comparing Figure 2 with Figure 6 shows that the trend of permeance with the variation of temperature does not follow the trend observed for the transmembrane flux since the transmembrane flux is increasing with temperature due to the increase in vapor pressure when the temperature increases. The effect of temperature on permeance can be interpreted via the activation energy. The activation energy of permeation is calculated by the logarithmic permeance

versus the inverse of the temperature. The calculated activation energy for the experiments is shown in Table 1. All activation energy of methanol and DMC permeation are negative (Table 1). The increase of temperature promotes the motion of polymer chains resulting in the expansion of the polymer free volume. Thus, it enhances the diffusion of permeant molecules through the membrane.[52] On the other hand, the heat of solution is the heat generated or absorbed during the sorption process, which depends on the sorption mechanisms dominated during sorption process. In this case, sorption is more dominant than diffusion in the process. As a consequence, increasing temperature is not favorable for the component to be adsorbed by the membranes, leading to a decrease of permeance.

The activation energy affects also the effect of temperature on the membrane permeation of a component. A larger absolute value of activation energy leads to a higher influence of temperature. From table 2, it can be observed that the membrane 1255-30 does not exhibit a large difference of activation energy on DMC and methanol. The membranes 4155-40 and 1255-50 have a higher absolute value of activation energy for DMC than for methanol, implying that temperature has a greater effect on DMC than on methanol for both membranes. On the other hand, the opposite is observed for membrane 4155-80, which will lead to a decrease of selectivity at high temperature.

Based on Figure 2 and Figure 6, it is observed that methanol shows higher values than dimethyl carbonate both in transmembrane flux and permeance. This high flux observation is caused by higher vapor pressure of methanol that leads to a higher driving force during the pervaporation separation, enhancing the transmembrane flux. Furthermore, methanol has also a higher permeance showing that the membrane material has a greater affinity for it. This gives an ideal situation in which the membrane enhances the effect of the – already favored – driving force for methanol, resulting in larger methanol flux.[50]

3.3 McCabe-Thiele separation diagram

In order to compare the advantage of using pervaporation with distillation, the McCabe-Thiele separation diagram is presented in this section for the studied mixture. In Figure 8, the concentration in the vapor phase (*i.e.,* permeate in pervaporation) is plotted versus the concentration in the liquid phase (*i.e.,* retentate in pervaporation). The comparison with distillation (dark points: DMC; blue points: methanol) is then straightforward. A flash distillation unit operated

316 at 85 °C and whose pressure is 1 atm is considered. Two main aspects should be considered: i) the
317 points close to the diagonal imply similar concentration in the liquid and vapor phase, thus, no
318 separation; and ii) if pervaporation points are not coincident to distillation points, it is due to the
319 effect of the membrane (if the points are coincident, the separation is due to the vapor-liquid
320 equilibrium).[50] The comparison of pervaporation and distillation gives additional information of
321 the merit or weakness of the membrane separation. It is shown that the membrane separation has
322 special advantage for separating methanol, the concentration of dimethyl carbonate (red) in the
323 permeate after pervaporation is lower than that in the flash equilibrium (black). The presence of
324 dimethyl carbonate in the permeate is decreased when comparing with flash equilibrium.

325 It is concluded that the membranes are selective to methanol and it is more concentrated in the
326 permeate. The points are far from the diagonal, therefore, an effective separation can be achieved.
327 In addition, the pervaporation points (red: DMC and pink: methanol) are not coincident to the
328 distillation points (black: DMC and blue: methanol) and the pervaporation points are further away
329 from the diagonal compared the distillation ones. This last point unambiguously proves the effect
330 of the membrane as well as the higher efficiency of pervaporation if compared to a simple
331 distillation.

332 As discussed above, pervaporation can be applied for the separation processes and it appears
333 advantageous in comparison with flash distillation. Moreover, it is also interesting that the
334 membranes reject glycerol and glycerol carbonate completely, as only methanol and dimethyl
335 carbonate are present in the permeate. In addition, different publications[25,26,53,54] describe
336 procedures that can achieve 97.7% - 99.93% conversion leading to a mixture containing glycerol
337 carbonate, DMC (in excess), methanol and a only residual glycerol. By removing DMC/methanol by
338 pervaporation instead of distillation, glycerol carbonate of high purity – but containing the traces
339 of glycerol – could be then obtained in a batch process. In addition, the permeate is a binary
340 mixture of methanol and DMC with high concentration of methanol (mole fraction of
341 methanol>0.84) obtained from only one pervaporation stage. Further purification and methanol
342 recovery may be the object of future research.

4. Conclusions

The application of pervaporation technology to separate a quaternary transesterification mixture consisting of glycerol, dimethyl carbonate, methanol and glycerol carbonate has been investigated using four commercial membranes. It was found that the studied membranes can reject glycerol and glycerol carbonate completely due to their low vapor pressure. The experimental results of permeance show that the use of these membranes enhances the permeation of methanol, which is the compound that has the highest transmembrane flux and has the largest driving force. Such a situation appears to be ideal as the membrane can operate under optimal conditions. In addition, the temperature shows great impact on the performance of membrane. When increasing the temperature, the flux increases, but the permeance decreases. Thus, working at low temperature is an advantage in terms of membrane performance. Regarding the McCabe-Thiele separation diagram analysis, it also shows that pervaporation can separate methanol more effectively than flash distillation. As consequence, pervaporation appears to be an alternative to improve the reaction yield by removing methanol from the reaction mixture and/or to break the azeotrope (methanol and DMC) as well as to remove glycerol and glycerol carbonate.

Acknowledgements

This research project was supported by the European Regional Development Fund (ERDF) and Wallonia within the framework of the program operational "Wallonie-2020.EU". The authors acknowledge the “Fonds européen de développement régional“ (FEDER) as well as the Wallonia (Belgium) for their financial supports via the “INTENSE4CHEM” projects (projects N° 699993-152208).

Appendix

A4. Hansen solubility parameter study

Solubility parameters, which was proposed by Hansen[58], has been widely applied predict the solubility of components into a polymer. This approach is to introduce three parameters: dispersion, polar and hydrogen bonding component. A sphere can be presented by these three dimensional parameters. The center of the sphere is determined by the polymer solubility parameters and its interaction radius, which could be found in the literature[59]. A polymer can be soluble in a solvent when solubility parameters of the solvent are located inside the polymer solubility sphere. The distance of the solvent from the center of the polymer solubility sphere can be calculated by following

equation[59]:

$$R_a = \left[4(\delta_{Ds} - \delta_{Dp})^2 + (\delta_{Ps} - \delta_{Pp})^2 + (\delta_{Hs} - \delta_{Hp})^2\right]^{1/2} \quad \text{(A4.1)}$$

where R_a is the distance of the solvent and the center of the sphere ($MPa^{1/2}$), and δ expresses as solubility parameters. The subscript *D*, *P* and *H* refer to dispersion, polar and hydrogen bonding component, respectively; and subscript *s* and *p* refer to solvent and polymer, respectively. If the distance between polymer and solvent ($\Delta\delta_{(s\text{-}p)}$) is smaller than the interaction radius, the polymer could be dissolved in this solvent. In this work, the active layer of commercial membrane composes of Polyvinyl alcohol (PVA) polymer with interaction radius of polyvinyl alcohol is 10.9. In addition, the Hansen solubility parameters of the mixture was estimated by equation (A4.2), proposed by Barton *et al.*[60]:

$$\overline{\delta_k} = \sum_i \phi_i \delta_{ki} \quad \text{(A4.2)}$$

where the subscripts *k* refers to D (dispersion component), P (polar component) and H (hydrogen bonding component), respectively). ϕ_i is the volume fraction of pure components in the mixture. The result of the calculation shows in table A4.

From table A4, it can be seen that the pure glycerol, glycerol carbonate and dimethyl carbonate are out of the solubility sphere, this shows that the PVA membrane is not favorable to sorb these components except methanol. In the work of Mulder et al.[61], preferential sorption can lead to the preferential permeation. Therefore, it can be predicted that methanol could have a high permeation in PVA membrane. In addition, it is important to calculate the solubility parameter of a mixture due to the variation of the solubility parameters of pure substances and causing coupling effect.[62] The result shows that the solubility parameters located within the PVA solubility sphere, therefore, the PVA membrane can sorb the components in the mixture and a potential coupling flux can occur.

A5. Reynolds number in the membrane cell estimation

In order to achieve turbulent flow, the Reynolds number should larger than 5000.

The kinematic viscosity of the mixture is estimated by the method proposed by Refutas (2000), which can estimate a mixture two or more liquids.

$$VBN_i = 14.534 \times \ln(\ln(\upsilon_i + 0.8)) + 10.975$$

where VBN_i is Viscosity Blending Number of each component.

The VBN of mixture is then calculated:

$$VBN_{mixture} = \sum_{i=0}^{N} x_i \times VBN_i$$

The kinematic viscosity of the mixture can be estimated using the viscosity blending number of mixture:

406 $$\upsilon_{mixture} = \exp\left(\exp\left(\frac{VBN_{mixture} - 10.975}{14.534}\right)\right) - 0.8$$

407 In our case, the kinematic viscosity is $2.16X10^{-6}$ m^2/s.

408 The flow velocity is 0.387 m/s for 70 L/h flow rate in our system and hydraulic diameter is 0.07 m.

409 Then the Reynolds number is calculated as follows:

410 $$Re = \frac{V_{feed\ fluid} \times D_H}{\upsilon_{mixture}} = 12550$$

411 Therefore, we introduce a high flow to minimize the resistance to mass transfer located at
412 boundary layer. Hence, it is assumed that the resistance to mass transfer located at boundary layer
413 can be negligible.

414

415

416 References

417 1. Abbaszaadeh, A., Ghobadian, B., Omidkhah, M. R. & Najafi, G. Current biodiesel production
418 technologies : A comparative review. *Energy Convers. Manag.* **63,** 138–148 (2012).
419 2. Lam, M. K., Lee, K. T. & Mohamed, A. R. Homogeneous , heterogeneous and enzymatic catalysis
420 for transesteri fi cation of high free fatty acid oil (waste cooking oil) to biodiesel : A review.
421 *Biotechnol. Adv.* **28,** 500–518 (2010).
422 3. Luo, X., Ge, X., Cui, S. & Li, Y. Bioresource Technology Value-added processing of crude glycerol
423 into chemicals and polymers. *Bioresour. Technol.* **215,** 144–154 (2016).
424 4. Quispe, C. A. G., Coronado, C. J. R. & Carvalho, J. A. Glycerol : Production , consumption , prices ,
425 characterization and new trends in combustion. *Renew. Sustain. Energy Rev.* **27,** 475–493 (2013).
426 5. Coronado, C. R., Carvalho, J. A., Quispe, C. A. & Sotomonte, C. R. Ecological efficiency in glycerol
427 combustion. *Appl. Therm. Eng. J.* **63,** 97–104 (2014).
428 6. Teng, W. K., Ngoh, G. C., Yusoff, R. & Aroua, M. K. A review on the performance of glycerol
429 carbonate production via catalytic transesterification : Effects of influencing parameters. *Energy*
430 *Convers. Manag.* **88,** 484–497 (2014).
431 7. Chai, S., Wang, H., Liang, Y. & Xu, B. Sustainable production of acrolein : investigation of solid
432 acid – base catalysts for gas-phase dehydration of glycerol. *Green Chem.* **9,** 1130–1136 (2007).
433 8. Godard, N. *et al.* High-Yield Synthesis of Ethyl Lactate with Mesoporous Tin Silicate Catalysts
434 Prepared by an Aerosol-Assisted Sol–Gel Process. *ChemCatChem* **9,** 2211–2218 (2017).
435 9. Claude, S. Research of new outlets for glycerol – recent developments in France. **101,** 101–104
436 (1999).
437 10. Jitrwung, R. & Yargeau, V. Biohydrogen and Bioethanol Production from Biodiesel-Based
438 Glycerol by Enterobacter aerogenes in a Continuous Stir Tank Reactor. *Int. J. Mol. Sci.* **16,** 10650–
439 10664 (2015).
440 11. He, Q. S., Mcnutt, J. & Yang, J. Utilization of the residual glycerol from biodiesel production for

renewable energy generation. *Renew. Sustain. Energy Rev.* **71,** 63–76 (2017).
12. Tshibalonza, N. N. & Monbaliu, J.-C. M. Revisiting the deoxydehydration of glycerol towards allyl alcohol under continuous-flow conditions. *Green Chem.* **19,** 3006–3013 (2017).
13. Monbaliu, J. C. M. *et al.* Effective production of the biodiesel additive STBE by a continuous flow process. *Bioresour. Technol.* **102,** 9304–9307 (2011).
14. Sonnati, M. O., Amigoni, S., Darmanin, T. & Choulet, O. Glycerol carbonate as a versatile building block for tomorrow: synthesis, reactivity, properties and applications. *Green Chem.* 283–306 (2013). doi:10.1039/c2gc36525a
15. Tin, G., Tat, K. & Teong, K. Recent development and economic analysis of glycerol-free processes via supercritical fl uid transesteri fi cation for biodiesel production. *Renew. Sustain. Energy Rev.* **31,** 61–70 (2014).
16. Aresta, M., Dibenedetto, A. & Bitonto, L. Di. New efficient and recyclable catalysts for the synthesis of di- and tri-glycerol carbonates. *RSC Adv.* **5,** 64433–64443 (2015).
17. Terence, W. T., Patti, A., Gates, W., Shaheen, U. & Sanjitha, K. Formation of glycerol carbonate from glycerol and urea catalysed by metal monoglycerolates. *Green Chem.* **15,** 1925–1931 (2013).
18. Vieville, C., Yoo, J. W., Pelet, S. & Mouloungui, Z. Synthesis of glycerol carbonate by direct carbonatation of glycerol in supercritical CO 2 in the presence of zeolites and ion exchange resins. *Catal. Lett.* **60,** 245–247 (1998).
19. Cho, H., Kwon, H., Tharun, J. & Park, D. Journal of Industrial and Engineering Chemistry Synthesis of glycerol carbonate from ethylene carbonate and glycerol using immobilized ionic liquid catalysts. *J. Ind. Eng. Chem.* **16,** 679–683 (2010).
20. Esteban, J., Domínguez, E., Ladero, M. & Garcia-ochoa, F. Kinetics of the production of glycerol carbonate by transesteri fi cation of glycerol with dimethyl and ethylene carbonate using potassium methoxide , a highly active catalyst. *Fuel Process. Technol.* **138,** 243–251 (2015).
21. José R. Ochoa-Gómez; Olga Gómez-Jiménez-Aberasturi; *et al.* Applied Catalysis A : General Synthesis of glycerol carbonate from glycerol and dimethyl carbonate by transesterification : Catalyst screening and reaction optimization. *Appl. Catal. A Gen.* **366,** 315–324 (2009).
22. Ramesh, S. & Debecker, D. P. Room temperature synthesis of glycerol carbonate catalyzed by spray dried sodium aluminate microspheres. *Catal. Commun.* **97,** 102–105 (2017).
23. Ilham, Z. & Saka, S. Esterification of glycerol from biodiesel production to glycerol carbonate in non‐catalytic supercritical dimethyl carbonate. *Springerplus* 1–6 (2016). doi:10.1186/s40064-016-2643-1
24. Stefanus, F. *et al.* Applied Catalysis A : General CaO-catalyzed synthesis of glycerol carbonate from glycerol and dimethyl carbonate : Isolation and characterization of an active Ca species. *"Applied Catal. A, Gen.* **401,** 220–225 (2011).
25. Okoye, P. U., Abdullah, A. Z. & Hameed, B. H. Journal of the Taiwan Institute of Chemical Engineers Glycerol carbonate synthesis from glycerol and dimethyl carbonate using trisodium phosphate. **68,** 51–58 (2016).
26. Hu, K., Wang, H., Liu, Y. & Yang, C. KNO3/CaO as cost-effective heterogeneous catalyst for the synthesis of glycerol carbonate from glycerol and dimethyl carbonate. *J. Ind. Eng. Chem.* **28,** 334–343 (2015).
27. Malyaadri, M., Jagadeeswaraiah, K., Prasad, P. S. S. & Lingaiah, N. Applied Catalysis A : General Synthesis of glycerol carbonate by transesterification of glycerol with dimethyl carbonate over

Mg / Al / Zr catalysts. *"Applied Catal. A, Gen.* **401,** 153–157 (2011).
28. Stefanus, F. *et al.* Applied Catalysis B : Environmental Synthesis of glycerol carbonate from the transesterification of dimethyl carbonate with glycerol using DABCO and DABCO-anchored Merrifield resin. *"Applied Catal. B, Environ.* **165,** 642–650 (2015).
29. Bai, R., Wang, S., Mei, F., Li, T. & Li, G. Journal of Industrial and Engineering Chemistry Synthesis of glycerol carbonate from glycerol and dimethyl carbonate catalyzed by KF modified hydroxyapatite. *J. Ind. Eng. Chem.* **17,** 777–781 (2011).
30. Pyo, S., Park, J. H., Chang, T. & Hatti-kaul, R. Greenhouse Gas Resources Research Group , Korea Research Institute of Chemical. *Curr. Opin. Green Sustain. Chem.* (2017). doi:10.1016/j.cogsc.2017.03.012
31. Stoian, D., Bansode, A., Medina, F. & Urakawa, A. Catalysis under microscope : Unraveling the mechanism of catalyst de- and re-activation in the continuous dimethyl carbonate synthesis from CO 2 and methanol in the presence of a dehydrating agent. *Catal. Today* **283,** 2–10 (2017).
32. Li, A. *et al.* Synthesis of dimethyl carbonate from methanol and CO 2 over Fe – Zr mixed oxides. *Biochem. Pharmacol.* **19,** 33–39 (2017).
33. Servel, C., Roizard, D., Favre, E. & Horbez, D. Improved energy efficiency of a hybrid pervaporation/distillation process for acetic acid production: Identification of target membrane performances by simulation. *Ind. Eng. Chem. Res.* **53,** 7768–7779 (2014).
34. Nagy, E., Mizsey, P., Hancs??k, J., Boldyryev, S. & Varbanov, P. Analysis of energy saving by combination of distillation and pervaporation for biofuel production. *Chem. Eng. Process. Process Intensif.* **98,** 86–94 (2015).
35. Luis, P., Amelio, A., Vreysen, S., Calabro, V. & Van der Bruggen, B. Simulation and environmental evaluation of process design: Distillation vs. hybrid distillation-pervaporation for methanol/tetrahydrofuran separation. *Appl. Energy* **113,** 565–575 (2014).
36. Smitha, B., Suhanya, D., Sridhar, S. & Ramakrishna, M. Separation of organic-organic mixtures by pervaporation - A review. *J. Memb. Sci.* **241,** 1–21 (2004).
37. Kujawa, J., Cerneaux, S. & Kujawski, W. Removal of hazardous volatile organic compounds from water by vacuum pervaporation with hydrophobic ceramic membranes. *J. Memb. Sci.* **474,** 11–19 (2015).
38. Sert, E. & Atalay, F. S. N-Butyl acrylate production by esterification of acrylic acid with n-butanol combined with pervaporation. *Chem. Eng. Process. Process Intensif.* **81,** 41–47 (2014).
39. Rathod, A. P., Wasewar, K. L. & Sonawane, S. S. Intensification of esterification reaction of lactic acid with iso-propanol using pervaporation reactor. *Procedia Eng.* **51,** 456–460 (2013).
40. Xu, S. & Wang, Y. Novel thermally cross-linked polyimide membranes for ethanol dehydration via pervaporation. *J. Memb. Sci.* **496,** 142–155 (2015).
41. Hiwale, R. S. Industrial Applications of Reactive Distillation : Recent Trends. *Int. J. Chem. React. Eng.* **2,** 1–52 (2004).
42. Luis, P., Degrève, J. & der Bruggen, B. Van. Separation of methanol-n-butyl acetate mixtures by pervaporation: Potential of 10 commercial membranes. *J. Memb. Sci.* **429,** 1–12 (2013).
43. Esteban, J., Ladero, M., Molinero, L. & García-ochoa, F. Chemical Engineering Research and Design Liquid – liquid equilibria for the ternary systems DMC – methanol – glycerol , DMC – glycerol carbonate – glycerol and the quaternary system DMC – methanol – glycerol carbonate – glycerol at catalytic reacting temp. *Chem. Eng. Res. Des.* **92,** 2797–2805 (2014).
44. Li, J. & Wang, T. Chemical equilibrium of glycerol carbonate synthesis from glycerol. *J. Chem.*

Thermodyn. **43,** 731–736 (2011).
45. Fredenslund, A., Gmehling, J. & Rasmussen, P. *Vapor-Liquid Equilibriums using UNIFAC. A Group-Contribution Method*. (Elsevier Scientific Pub. Co., New York, 1977).
46. Klopffer, M. H. & Flaconnèche, B. Transport Properties of Gases in Polymers : Bibliographic Review. *Oil gas sci. technol.* **56,** 223–244 (2001).
47. Feng, X. & Huang, R. Y. M. Estimation of activation energy for permeation in pervaporation processes. *J. Memb. Sci.* **118,** 127–131 (1996).
48. Jyoti, G., Keshav, A. & Anandkumar, J. Review on Pervaporation : Theory , Membrane Performance , and Application to Intensification of Esterification Reaction. *J. Eng.* **2015,** 24 (2015).
49. Liu, J., Ma, Y., Hu, K., He, H. & Shao, G. Pervaporation separation of isopropanol/benzene mixtures using inorganic-organic hybrid membranes. *J. Appl. Polym. Sci.* **117,** 2464–2471 (2010).
50. Luis, P. & Van Der Bruggen, B. The driving force as key element to evaluate the pervaporation performance of multicomponent mixtures. *Sep. Purif. Technol.* **148,** 94–102 (2015).
51. Villaluenga, J. P. G., Khayet, M., Godino, P., Seoane, B. & Mengual, J. I. Pervaporation of Toluene / Alcohol Mixtures through a Coextruded Linear Low-Density Polyethylene Membrane. *Ind. Eng. Chem. Res.* **42,** 386–391 (2003).
52. Aminabhavi, M. & Phayde, H. T. S. Sorption/diffusion of aliphatic esters into tetrafluoroethylene/propylene copolymeric membranes in the temperature interval from 25 to 70 °C. *Eur. Polym. J.* **32,** 1117–1126 (1996).
53. Wang, S. *et al.* Applied Catalysis A , General Synthesis of glycerol carbonate from glycerol and dimethyl carbonate catalyzed by calcined silicates. *Appl. Catal. A, Gen.* **542,** 174–181 (2017).
54. Wang, H., Pang, L., Yang, C. & Liu, Y. Production of glycerol carbonate via reactive distillation and extractive distillation : An experimental study. *CJCHE* **23,** 1469–1474 (2015).
55. Wei, H. *et al.* Design and Control of Dimethyl Carbonate − Methanol Separation via Pressure-Swing Distillation. *Ind. Eng. Chem. Res.* **52,** 11463–11478 (2013).
56. Hu, C. C. & Cheng, S. H. Development of alternative methanol/dimethyl carbonate separation systems by extractive distillation — A holistic approach. *Chem. Eng. Res. Des.* **127,** 189–214 (2017).
57. Wang, L., Li, J., Lin, Y. & Chen, C. Separation of dimethyl carbonate / methanol mixtures by pervaporation with poly (acrylic acid)/ poly (vinyl alcohol) blend membranes. *J. Memb. Sci.* **305,** 238–246 (2007).
58. Hansen, C. M. 50 Years with solubility parameters — past and future. *Prog. Org. Coat.* **51,** 77–84 (2004).
59. Hansen, C. M. *Hansen Solubility Parameters -A User's Handbook*. (CRC Press, 2007).
60. Barton, A. F. M. Solubility Parameters. *Chem. Rev.* **75,** 731–753 (1975).
61. Mulder, M. H. V., Franken, T. & Smolders, C. A. Preferential sorption versus preferential permeability in pervaporation. *J. Memb. Sci.* **22,** 155–173 (1985).
62. Li, W. & Luis, P. Understanding coupling effects in pervaporation of multi-component mixtures. *Sep. Purif. Technol.* **197,** 95–106 (2018).

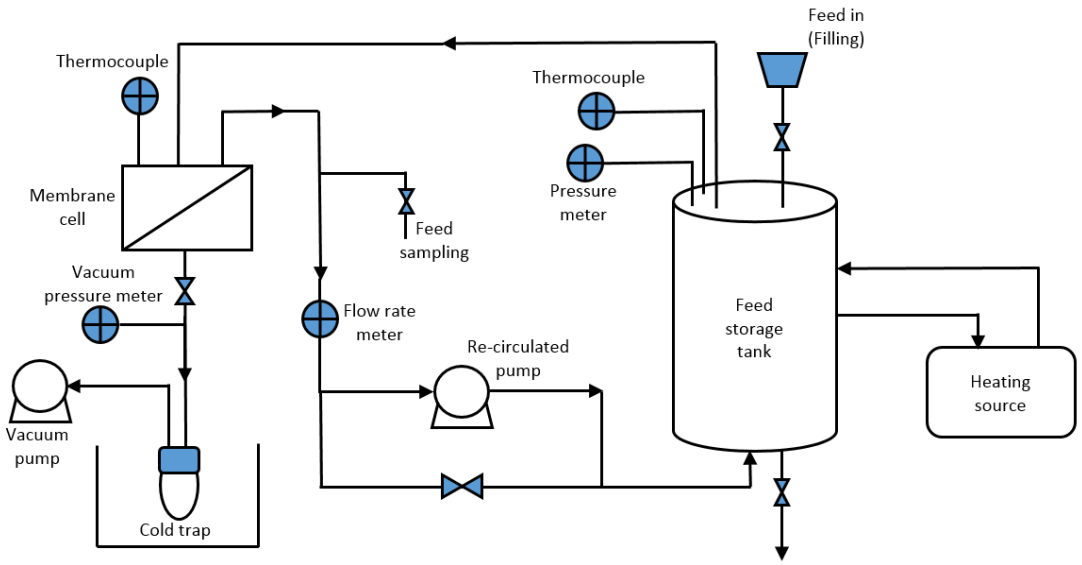

Figure 1. Schematic representation of the pervaporation experimental equipment

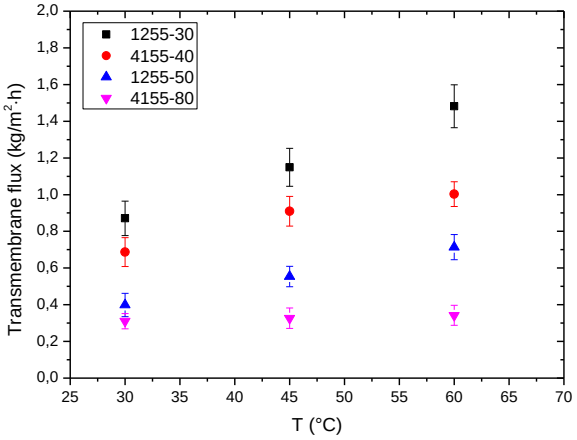

Figure 2. Overall transmembrane flux of each membrane at different temperatures

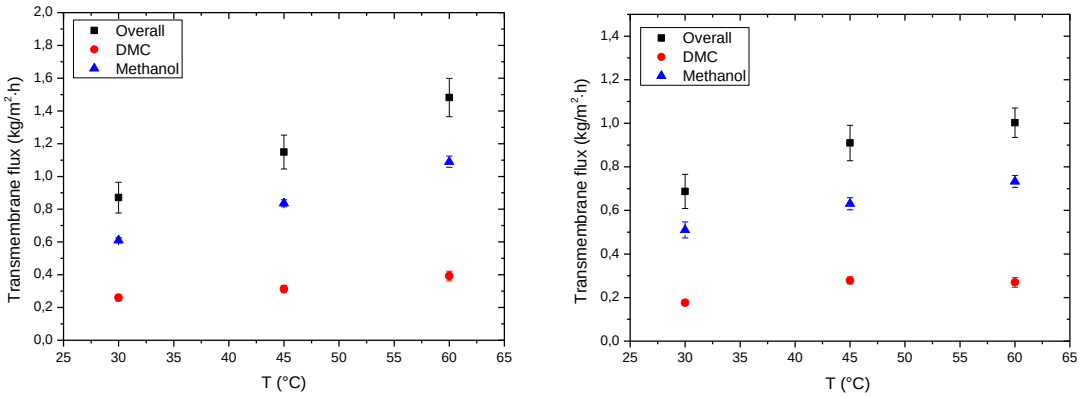

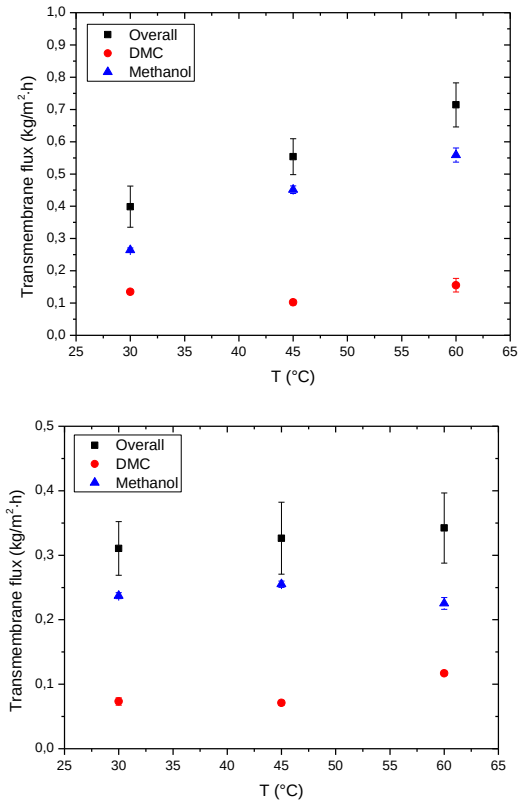

Figure 3. Partial flux of each component of each membrane at different temperatures: (a) membrane 1255-30 ; (b) membrane 4155-40 ; (c) membrane 1255-50, and (d) membrane 4155-80.

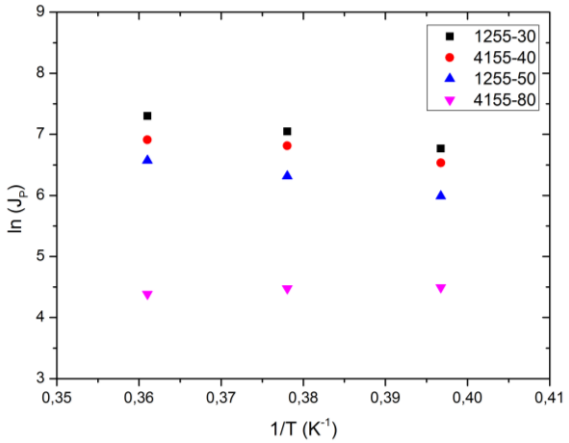

Figure 4. Dependence of lnJ_P vs. 1/T of four commercial membranes

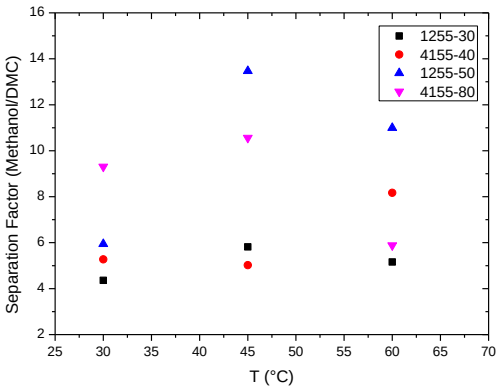

Figure 5. Separation factor of methanol/DMC of different types of membranes at different temperature

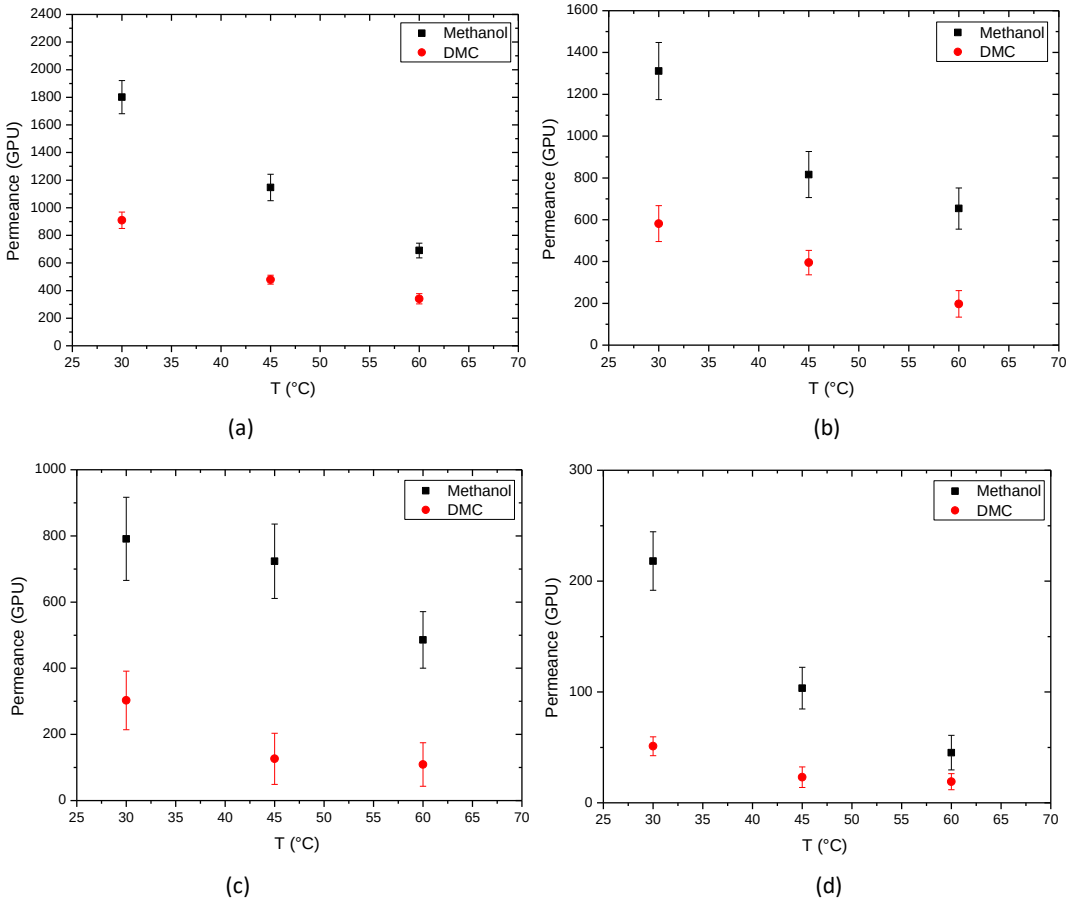

Figure 6. The permeance of different types of membranes at different temperature (a) 1255-30 membrane, (b) 4155-40 membrane, (c) 1255-50 membrane and (d) 4155-80 membrane

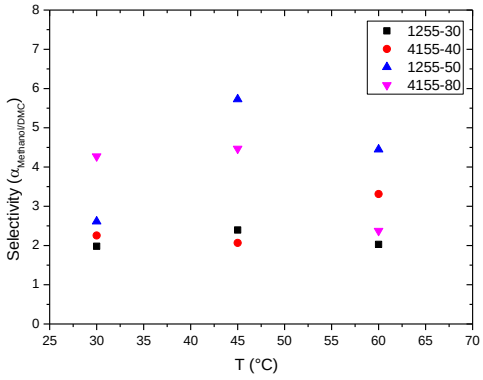

Figure 7. Selectivity of methanol/DMC of different types of membranes at different temperature

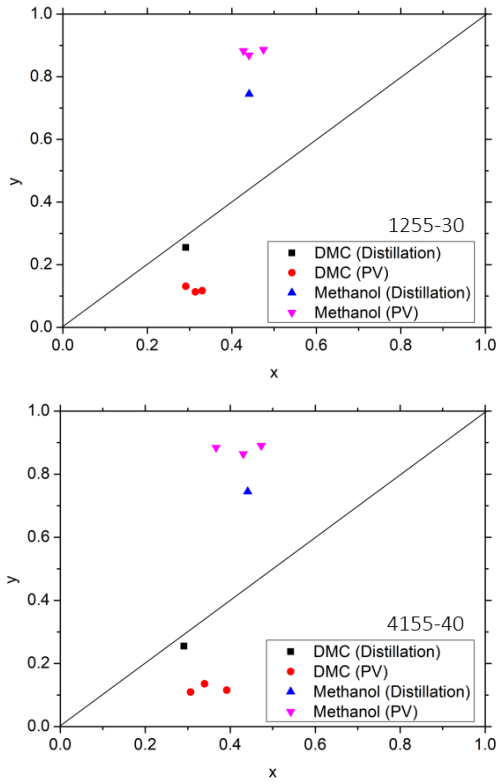

(a) (b)

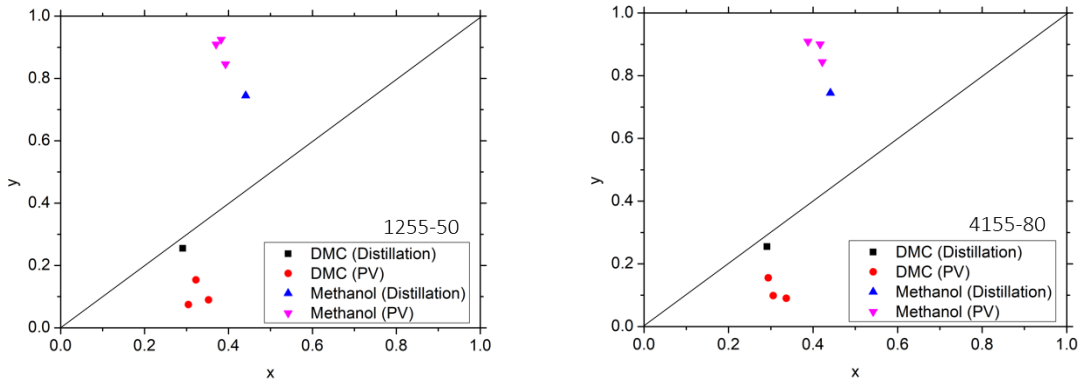

(c) (d)

Figure 8. McCabe-Thiele separation diagram that shows the pervaporation selectivity for each compound using the membranes: a) 1255-30, b) 4155-40, c) 1255-50 and d) 4155-80. The axis x and y are given in molar fraction. The three points shows the effect of temperature at 30 °C, 45 °C and 60 °C. The black and blue symbols correspond to the separation obtained by simulation of flash equilibrium at 85 °C (glycerol and glycerol carbonate are not observed in the vapor phase due to their high boiling point).

650
651
652 Table 1. Activation energy of methanol and DMC for the different commercial membranes

Activation energy (KJ/mol)		
Membrane	DMC	Methanol
1255-30	-27,6 ± 1.35	-26,8 ± 2.22
4155-40	-30,1 ± 1.52	-19,6 ± 1.63
1255-50	-28,8 ± 1.54	-13,5 ± 1.69
4155-80	-27,8 ± 1.49	-44,0 ± 1.43

653
654
655
656
657
658

Appendix

A1.

Table A1. The vapor pressure (atm) of each component at 30 °C, 45 °C and 60 °C.

Temperature (°C)	Methanol	Glycerol	Dimethyl carbonate	Glycerol carbonate
30	0.2176	$4.0467X10^{-7}$	0.0945	$2.5165X10^{-7}$
45	0.4449	$2.1291X10^{-6}$	0.1883	$9.8592X10^{-6}$
60	0.7854	$7.9620X10^{-6}$	0.3253	$3.2775X10^{-6}$

A2.

Table A2. Activity coefficient of each component at 30 °C, 45 °C and 60 °C.

Temperature (°C)	Methanol	Glycerol	Dimethyl carbonate	Glycerol carbonate
30	1.232	1.925	1.616	1.108
45	1.223	1.885	1.575	1.100
60	1.216	1.853	1.528	1.091

A3.

Table A3. The driving force of methanol and dimethyl carbonate of each membrane at 30 °C, 45 °C and 60 °C.

Membranes	Temperatures	Methanol	Dimethyl carbonate
1255-30	30	0.0867	0.0260
	40	0.1866	0.0593
	50	0.4038	0.1047
4155-40	30	0.0996	0.0276
	40	0.1978	0.0641
	50	0.2869	0.1243
1255-50	30	0.0853	0.0404
	40	0.1596	0.0736
	50	0.2943	0.1293
4155-80	30	0.0801	0.0376
	40	0.1702	0.0755
	50	0.2985	0.1307

A4.

Table A4. Calculated Hansen solubility parameters of each component/mixture and R_a

Material	**δ_D**	**δ_P**	**δ_H**	**$\Delta\delta_{(s-p)}$**
PVA	17.2	13.6	15.4	

Glycerol	17.4	12.1	29.3	13.99
Glycerol carbonate	17.9	25.5	17.4	12.15
Methanol	15.1	12.3	22.3	8.18
Dimethyl carbonate	15.5	3.9	9.7	11.75
Mixture	16.2	12.4	16.8	2.79

678
679
680